JEODEZİ VE JEOİNFORMASYON DERGİSİ
JOURNAL OF GEODESY AND GEOINFORMATION
ISSN : 2147-1339
e-ISSN: 2667-8519

Araştırma Makalesi / *Research Article*
Yıl / *Year:* 2024 **Cilt** / *Volume:* 11 **Sayı** / *Issue*: 1
Sayfa / *Page*: 41-50
Dergi No / *Journal No*: 119
Doi: 10.9733/JGG.2024R0004.E

Examining the accuracy of DEM of difference and 3D point cloud comparison methods: Open pit mine case study

Nilufer Ozdas[1], Mehmet Guven Kocak[2*], Serkan Karakis[2]

[1]*İzmir Kâtip Çelebi University, Institute of Science, Geomatics Engineering, Çiğli, İzmir, Türkiye.*

[2]*İzmir Kâtip Çelebi University, Faculty of Engineering and Architecture, Department of Geomatics Engineering, Çiğli, İzmir, Türkiye.*

Abstract: *With the widespread use of unmanned aerial vehicles (UAV), high-accuracy photogrammetric mapping studies can be carried out over small areas with cost-effective simple systems. By comparing images obtained at different epochs, 3 Dimensional (3D) change detection studies can be easily performed. Digital surface models (DSM) are obtained from the point cloud (PC) with the processing software, their differences are taken, and temporal changes can thus be modeled. This method is known as DEM (DSM) of Difference (DoD) in practice and has low computational cost. Recently, with the availability and accessibility of powerful computers capable of processing increasing amounts of data, 3D change detection studies can be performed directly with raw PCs without converting them to DSM. Methodologically, DoD and PC-based analysis strategies have different evaluation stages and outputs. With DoD, only changes in the vertical direction can be revealed, while PC comparison methods can produce the 3D change vector. In this study, the well-established DoD method and Multiscale Model-to-Model Cloud Comparison (M3C2), one of the 3D PC comparison methods, were compared. The accuracy of the methods was tested at an active open pit mine site where intensive excavation works have been undertaken. Standard deviation values were found below 11 cm with M3C2 distance and DoD differences obtained from UAV images having average ground sampling distances (GSD) of 5.8-6.9 cm. Only about 1% of the differences were categorized as outliers.*

Keywords: 3D point cloud, Digital surface modeling, DEM of difference, M3C2, Accuracy

Fark SYM ve 3B nokta bulutu karşılaştırma yöntemlerinin doğruluklarının incelenmesi: Açık maden ocağı örneği

Öz: *İnsansız hava araçlarının (İHA) yaygınlaşmasıyla birlikte düşük maliyetli basit sistemlerle küçük alanlar üzerinde yüksek doğruluklu fotogrametrik haritalama çalışmaları yapılabilmektedir. Farklı zamanlarda elde edilen görüntüler karşılaştırılarak 3 Boyutlu (3B) değişim tespit çalışmaları da kolaylıkla gerçekleştirilebilmektedir. Fotogrametrik değerlendirme yazılımları ile elde edilen nokta bulutundan sayısal yüzey modelleri (SYM) elde edilir, farkları alınır ve zamansal değişimler modellenebilir. Bu yöntem pratikte Fark SYM yöntemi olarak bilinir ve düşük hesaplama maliyetine sahiptir. Son zamanlarda, büyük veri işleyebilen güçlü bilgisayarların gelişmesi ve bunlara erişimin düşük maliyetlerle mümkün olması neticesinde 3B değişim tespit çalışmaları ham nokta bulutundan SYM elde edilmeksizin doğrudan noktaların kendisiyle yapılabilmektedir. Metodolojik olarak, Fark SYM ve nokta bulutu tabanlı analiz stratejilerinin farklı değerlendirme aşamaları ve çıktıları vardır. Fark SYM ile sadece düşey yöndeki değişimler ortaya çıkarılabilirken, ham nokta bulutu karşılaştırma yöntemleri 3B değişim vektörünü hesaplayabilmektedir. Bu çalışmada, pratikte sıklıkla kullanılan Fark SYM yöntemi ile 3B nokta bulutu karşılaştırma yöntemlerinden biri olan M3C2 karşılaştırılmıştır. Yöntemlerin doğruluğu, yoğun kazı çalışmalarının yapıldığı aktif bir açık ocak maden sahasında test edilmiştir. Ortalama yer örnekleme aralığı 5.8-6.9 cm olan İHA görüntülerinden elde edilen M3C2 uzunluk ve DoD farklarıyla 11 cm'den düşük standart sapma değerleri bulunmuştur. Farkların sadece %1 civarındaki kesimi uyuşumsuz olarak ortaya çıkmıştır.*

Anahtar Sözcükler: 3B nokta bulutu, Sayısal yüzey modeli, Fark SYM, M3C2, Doğruluk

* Sorumlu Yazar/Corresponding Author: Tel: +90 232 329 3535 / 3775

Geliş Tarihi/Received: 15.01.2024
Kabul Tarihi/Accepted: 28.02.2024

0009-0007-3929-6813, niluferozdass@gmail.com (Ozdas N.)
0000-0002-7992-5860, mehmetguven.kocak@ikcu.edu.tr (Kocak M.G.)*
0000-0002-5765-7666, serkan.karakis@ikcu.edu.tr (Karakis S.)

1. Introduction

The earth's surface is in a state of constant change. Changes can be of natural origin as in earthquakes, landslides, etc., or anthropogenic in the form of mining or urbanization (Cao et al., 2023; Ren et al., 2019). Revealing change over time is important for inventory mapping, planning, and other retrospective studies aiming to understand the phenomena under investigation. Depending on the nature of the problem and the desired accuracy, change detection can be performed with point (e.g. GNSS deformation studies) and surface data (photogrammetric and remote sensing imagery) (Cook, 2017). While the first digital change detection studies in remote sensing were of 2 Dimensional origin, 3 Dimensional (3D) change detection studies have started to increase parallel to the developments in carrier platform, sensor, and computer technologies (Okyay et al., 2019; Théau, 2022).

Data acquisition can be provided by satellite, airborne, and unmanned aerial vehicle (UAV) platforms for change detection studies. However, airborne and UAV systems seem to be highly flexible for quick data capture providing high temporal resolution as well as high spatial resolution (Nex et al., 2022). In terms of endurance, airborne imaging is used to obtain data from larger areas, while UAVs are opted for imaging smaller areas due to their low battery life. Practitioners benefit from photogrammetric and LiDAR sensors attached to a UAV. However, the choice of imaging device is made for photogrammetric cameras since LiDAR implementation costs more and cannot be deployed on small UAVs. Thus, UAV photogrammetry can be operated easily and provides high spatial and temporal resolution imagery at low cost.

Whether acquired with LiDAR or a camera, the data set produced is a dense point cloud (PC). For change detection, the PC acquired in multiple epochs needs to be further processed. The preferred approach for evaluation depends on whether additional data processing is applied to the raw PC or not. There are four standard methods for extracting change information from reference and target PCs (de Gélis et al., 2021; Kharroubi et al., 2022; Li et al., 2024). These are cloud-to-cloud (C2C), cloud-to-mesh (C2M), multiscale model-to-model cloud comparison (M3C2), and DEM of difference (DoD). C2C compares cloud points across two epochs and does not require any additional data processing (Besl & McKay, 1992). C2M searches for the correspondence of the points in the reference PC and the mesh obtained from the target cloud. In the M3C2 method, the distance between the surface normal created at a point in the reference point cloud and the surface created in the target PC is estimated. The DoD approach requires more processing steps than the other three approaches, but it is more advantageous than these three methods in terms of processing time. Here, digital surface models (DSM) obtained at different epochs are compared grid by grid. To generate DSMs, it is necessary to form a triangular irregular network (TIN) by applying a triangulation algorithm to each PC and then interpolating the height value for each grid in the specified grid interval using the TIN surface (Wilson, 2012).

The most important feature of C2C, C2M, and M3C2 methods is that they can model the change between reference and target PCs as a vector. Unlike these methods, DoD can only reveal the change in the vertical direction. Few studies have undertaken simultaneous accuracy assessment of M3C2 and DoD approaches. For example, Nourbakhshbeidokhti et al. (2019) compared four methods including M3C2 and DoD approaches with reference data in the context of topographic and volumetric changes in channel sedimentation. Liu et al. (2023) determined the accuracy of the methods on 0.5 and 0.8 km long profiles using GPS measurements within a mining-induced subsidence monitoring project. In these studies, the two methods were compared indirectly using ground truth data in a limited part of the study areas. To the best of our knowledge, no study attempted to quantify the direct difference of both methods across a larger area, e.g. covering the entire study area. Thus, this study aims to compare the accuracies achieved by M3C2, which is the most effective of the three methods based on the processing of PCs to determine the change, and DoD, which is more optimal in terms of computation time.

2. Method

2.1 Study Area

The study area is located between 39.12521-39.13422N and 27.57405-27.58744E degrees and within the borders of Soma district of Manisa province, Türkiye. The heights of the area above the mean sea level vary between 680-865 m. The open pit mine field covers an area of 2.4 km^2 in total, where mining activities were first initiated in August 2021. The common area covered by the DSMs for the three epochs used in this study is 0.8 km^2. A landslide occurred in the north of the study area, and this was recorded in the last epoch survey. The fact that the area was hit by a landslide in addition to the change caused by mining activities played an important role in the selection of the area for a case study.

2.2 Data Processing

The study compares the reference DSM obtained from imagery at Epoch 0 (August 3, 2021) with the target DSMs generated for two distinct epochs. Epoch 1 images were taken at a temporally close (21 days) and Epoch 2 at a distant (256 days) interval from the reference Epoch 0. In all three epochs, images were acquired using a DJI Phantom UAV with the FC6310S camera model having a focal length of 8.8 mm and a square pixel size of 2.41 µm. The numerical data of the flights are presented in Table 1.

Table 1: *Flight data for images used in the study*

UAV Campaign	Days from the 0^{th} Epoch	Total Images	Altitude [m]	Mean Ground Sampling Distance (GSD) [cm]	Area [km^2]
Epoch 0 Aug2, 2021	0	401	270	6.9	1.86
Epoch 1 Aug23,2021	21	454	220	5.8	0.80
Epoch 2 Apr15,2022	256	587	230	5.8	2.42

Epoch 1 survey covers the smallest area as mining operations were concentrated to a limited section within 21 days after the excavation started in August 2021. In the 256 days after Epoch 0, activities spread over a wider area, so the imaging also covers a larger area. However, to make an effective comparison within the scope of the study, Epoch 1 covering the smallest area, was taken as the basis and the other two data sets were truncated to cover the area bounded by this area.

Photogrammetric orientations of the images were performed with Agisoft Photoscan software. After the image matching and relative orientation stages, dense matching was performed and PCs to be used in DSM production were obtained. The absolute orientation of the model was made by ground control points (GCP) and its check was conducted by independent check points (ICP). The coordinates of the control points were determined separately for each of the three epochs using GNSS relative positioning where a fixed station established in the field was taken as reference.

DSMs with 0.5 m grid spacing were produced with the PCs obtained after the photogrammetric dense matching stage. Inverse Distance Weighting (IDW) was preferred as the interpolation method. 3x3 dimensional low pass filtering was applied to the raw DSMs. The DSMs to be used in the comparison were thus made ready for DoD.

The other method used in the study is based on the comparison of 3D PCs at different epochs and finding the distance vector between the reference and target PCs. The M3C2 approach is used to compare PCs and the method works in two stages (URL-1). The working principle of the method is illustrated in Figure 1. In the first stage, a plane is estimated with the help of the points within the circle of diameter D created at a selected point in the reference PC, and the normal direction of this

plane is calculated. In the second stage, the average position for each cloud is found with the reference and compared points inside the cylinder of diameter d formed in the direction of the normal. In this way, the distance between the two average positions is obtained as the change vector (Lague et al., 2013).

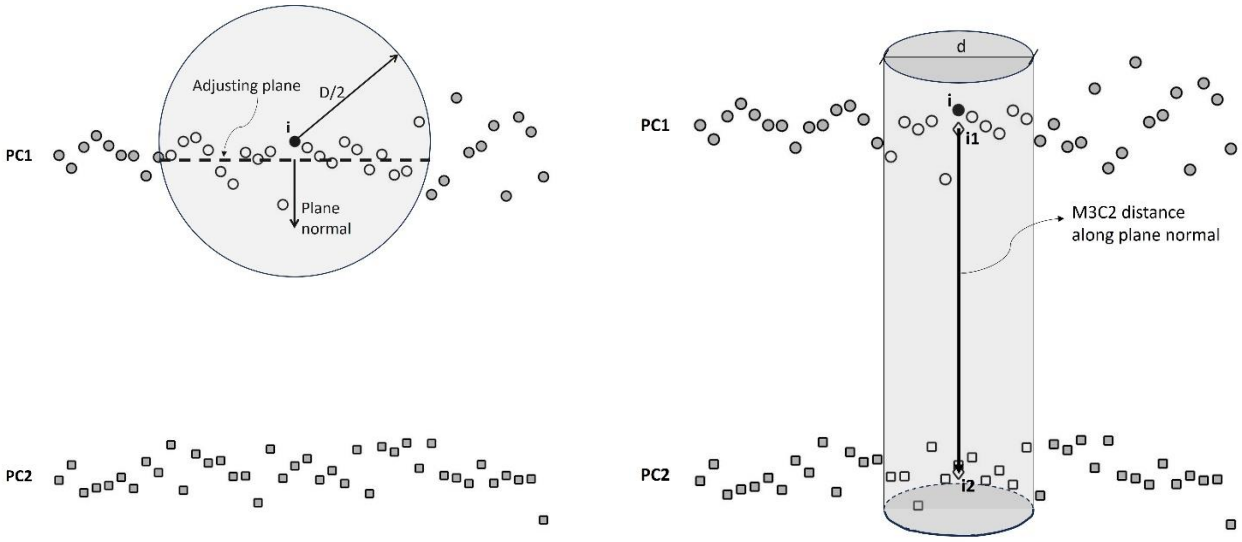

Figure 1: *Visual illustration of the M3C2 method (The figure in Lague et al. (2013) is slightly modified)*

2.3 DoD and M3C2 Comparison

DoD is based on the principle of taking the algebraic differences of DSMs and obtaining the changes in the vertical direction (Williams, 2012). M3C2, on the other hand, uses a 3D point cloud to extract the difference vector between a point in the reference DSM cloud and its corresponding point in the compared DSM. Therefore, it is not possible to directly compare DoD and M3C2 results. To make a comparison, 3D coordinates of the corresponding point in the compared cloud must be found. For this, the 3D unit vector components n_X, n_Y, and n_Z and the distance value generated by M3C2 can be used. Using the unit vectors;

$$n_{XY} = \sqrt{n_X^2 + n_Y^2} \tag{1}$$

$$A = \tan^{-1}\left(\frac{n_Y}{n_X}\right) \tag{2}$$

$$Z = \tan^{-1}\left(\frac{n_{XY}}{n_Z}\right) \tag{3}$$

azimuth and zenith angles are calculated. The transformation from polar to cartesian coordinates is performed by the following equations:

$$X_{Compared} = X_{Ref} + d \cdot \sin Z \cdot \cos A \tag{4}$$

$$Y_{Compared} = Y_{Ref} + d \cdot \sin Z \cdot \sin A \tag{5}$$

$$Z_{Compared} = Z_{Ref} + d \cdot \cos Z \tag{6}$$

Using the horizontal components (X, Y), the vertical component in the compared DSM is interpolated (Z_{int}). This height is then compared with the M3C2 height in the compared DSM ($Z_{Compared} - Z_{int}$).

The second comparison is designed according to the DoD approach. To facilitate this comparison, both DSMs were sampled at the production stage to correspond to the same grid node coordinates. Thus, a point taken on both DSMs and DoD corresponds to the same point horizontally on all three gridded surfaces. The comparison is based on whether the M3C2 reference and compared PC points are in the same DoD grid. In the obtained M3C2 solution, the points meeting this condition were separated and the M3C2 distance and DoD values at these points were compared.

3. Results and Discussion

Photogrammetric PCs were obtained with the processing software and the number of cloud points exceeded 10.3, 15.2, and 16.2 million for Epochs 0, 1, and 2, respectively. Triangulation and interpolation steps were applied to these point clouds to obtain DSMs with 0.5 m grid spacing (Figure 2). During the calculation of DSMs, vegetation areas were manually demarcated and excluded from the computation.

In the M3C2 assessment, subsampling of the reference PC was performed at 1 m intervals for reducing computation time and projection parameters were set as D=0.14 m and d=0.28 m. As can be seen, the parameters were set to 2 and 4 pixels respectively, so that the results are not affected by abrupt height changes, especially in areas close to the excavation boundaries. Epoch 0 was set as reference and correspondence of subsampled points at the other two epoch solutions were searched for. While Epoch 1 comparison delivered distances at all subsample points, M3C2 distances could be obtained for 67% of the extracted 500k Epoch 2 points. This can be explained by the fact that image matching in Epoch 2 generated fewer points in the excavated flat areas. Excavation works in Epoch 1 imaging time did not advance considerably; thus, better image matching was achieved in Epoch 1 than in Epoch 2 (Figure 3).

In order to compare DoD and M3C2 results, it is important to determine the accuracy of the height component. Threshold values for the statistical tests used in the comparisons were determined based on this accuracy value. In this context, the points whose coordinates were obtained by the GNSS method were divided into two subsets. GCPs were used for the estimation of the model's absolute orientation parameters and the remaining ICPs were used for model validation. As can be seen in Table 2, where the results of all three epochs are given, the values obtained with GCPs are more optimistic, while ICP results are more realistic when the ground sampling distance is considered (see Table 1).

Table 2: *Accuracy values attained for each survey. X, Y, and Z coordinates are given in the WGS84 datum*

Epoch	Number of GCPs /ICPs	RMSE XY [cm] GCPs / ICPs	RMSE Z [cm] GCPs / ICPs
0	11 / 8	1.2 / 8.6	1.6 / 8.6
1	7 / 8	3.3 / 3.6	1.5 / 4.7
2	13 / 15	2.6 / 4.7	1.7 / 8.2

Here, although the Z component accuracy obtained with ICP in Epoch 1 was the best, the accuracies in the other two epochs were close to each other. To make a realistic comparison, the RMSE value of the reference epoch was adopted for each DSM's vertical component accuracy, which is the worst accuracy value obtained with ICP. In the case of comparing two different DSMs, the absolute threshold value is computed as $1.96 \cdot \sqrt{2} \cdot RMSEZ = 23.8$ cm at 95% confidence level by applying error propagation with independence assumption of the variables (James et al., 2017). The threshold value is found 33.7 cm for comparing the height difference of two values. These values are adopted as the acceptance/rejection boundary to decide whether the difference values are significant in the comparisons made.

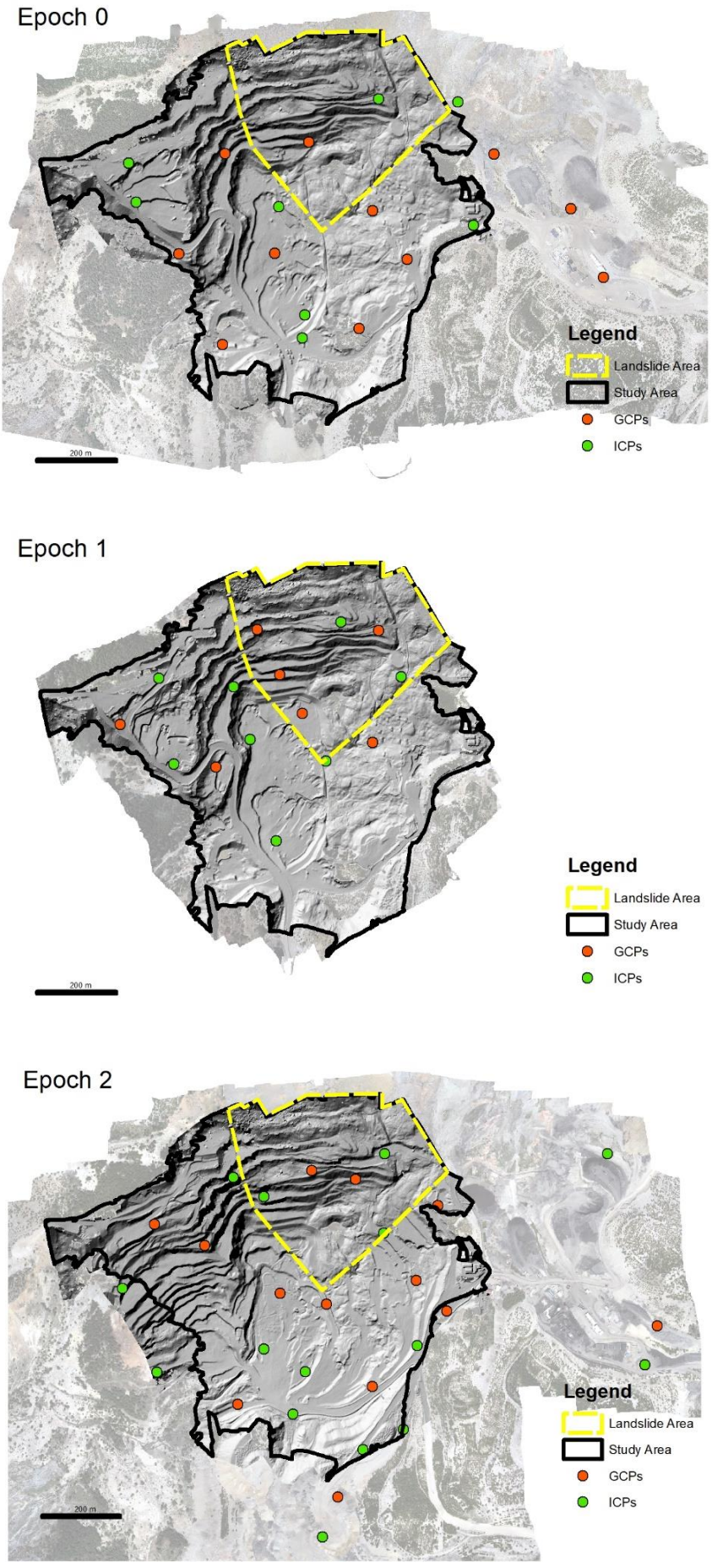

Figure 2: *DSMs generated from photogrammetric PCs*

The M3C2 solution delivers the 3D coordinates of the points in the reference epoch together with the 3D unit vectors and distance values of the change direction to the compared PC. The new 3D position of the changed point $(X, Y, Z)_{Compared}$ in the comparison PC is calculated by vector and distance values. The compared DSM value at this location was obtained by interpolation (Z_{int}) using the calculated horizontal components $(X, Y)_{Compared}$. The comparison results ($Z_{int} - Z_{Compared}$) for both epochs are presented in Table 3. The standard deviation values calculated with height differences for both epochs were close to each other. Outliers exceeding the threshold value of 23.8 cm in the comparison of the two data sets make up a small fraction of the entire data sets. Therefore, it can be said that although M3C2 and DOD offer different solution sets, they perform change detection for this study area successfully.

Table 3: *M3C2 vs DSM comparison of heights*

Data Set	Number of M3C2 Points	min / mean / max [m]	Std. Dev. of Differences [cm]	Number of Outliers / Percentage
Epoch 1	413 871	-6.45 / 0.01 / 12.81	10.8	6185 / 1.5 %
Epoch 2	366 893	-7.35 / 0.05 / 12.47	8.9	2676 / 0.7 %

For carrying out the second comparison, M3C2 points satisfying a condition were selected. This condition states that the start and end points of the distance vector found with the M3C2 solution must be within the same DoD grid. For this purpose, the geographical left and top extent values of all DSMs were initially set to the same value, so that the same grid nodes in each DSM show identical horizontal coordinates. M3C2 distance values and grid DoD values meeting this condition were compared. The numerical data of this comparison is presented in Table 4.

Table 4: *M3C2 distance values vs DoD*

Data Set	Number of Points / Percentage	min / mean / max [m]	Std. Dev. of Differences [cm]	Number of Outliers / Percentage
Epoch0 – Epoch1	346 320 / 83.7%	-1.94 / 0.025 / 4.83	8.6	2653 / 0.8%
Epoch0 – Epoch2	131 818 / 31.9%	-1.80 / -0.024 / 3.21	10.7	1544 / 1.2%

Difference values exceeding the threshold value of 33.7 cm were labeled as outliers and removed from the dataset. In Epoch 1, 83.7 of the total PC points fulfill the condition of being within the same DoD grid, while this ratio drops below one-third of all PC points obtained for Epoch 2. In Epoch 1 data taken 21 days after the mining activities started, a higher percentage of points could be obtained since the excavation works did not progress. On the other hand, fewer points could be evaluated in Epoch 2 data since excavation works spread over larger areas within 256 days and a landslide occurred on the site (Figure 3).

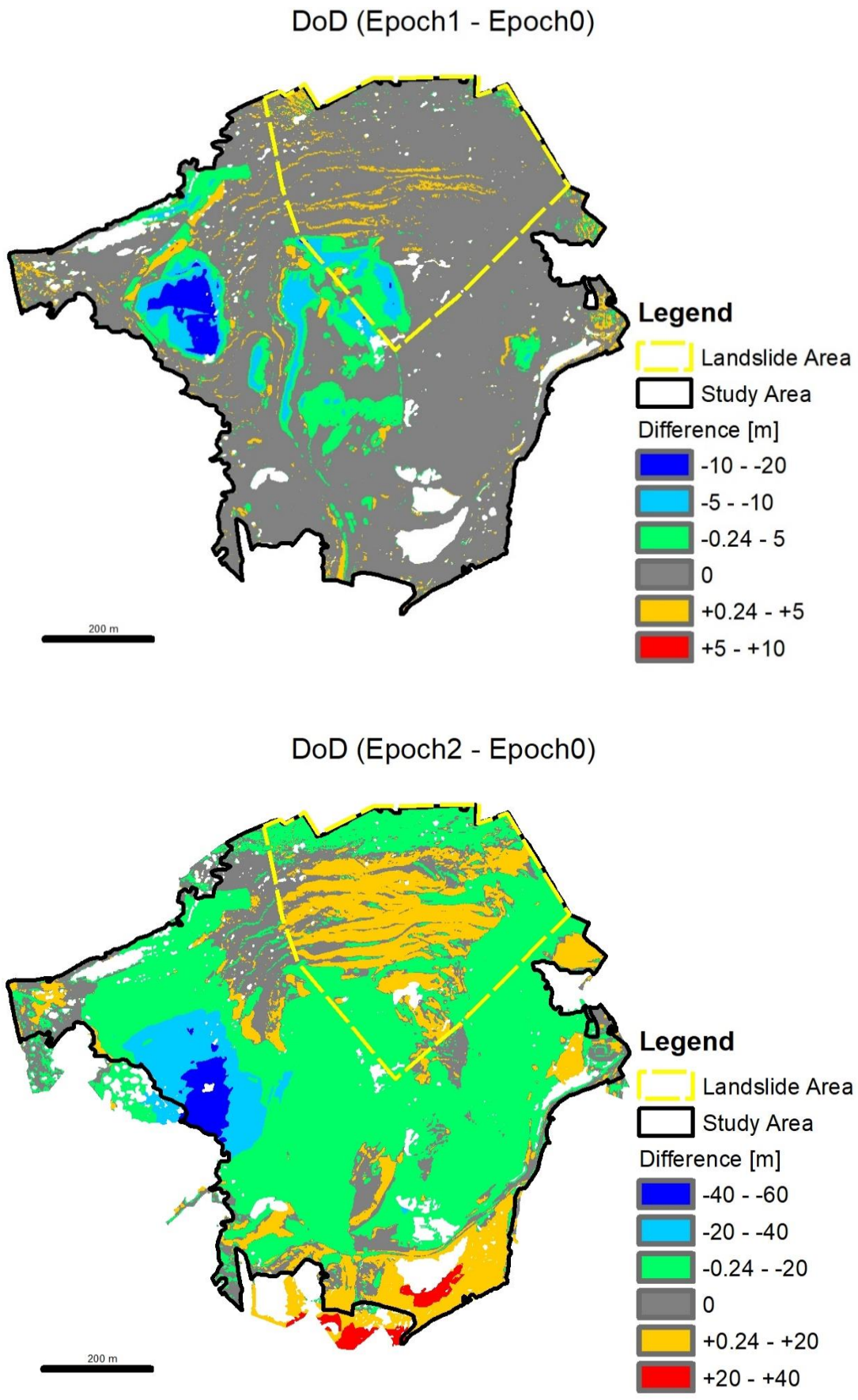

Figure 3: *DoDs with reference to Epoch 0. Note separate difference scale for each plot.*

4. Conclusion

In this study, two change detection methods, DoD and M3C2, are compared in an open pit mine case. A direct one-to-one comparison of the two methods is not possible given their outputs. For this reason, the coordinates of the distance vector produced by M3C2 and the corresponding point in the compared PC were calculated, and the DSM height values were interpolated with the calculated horizontal position values. The calculated and interpolated values were then compared. A second comparison was made with a limited set of points within the same DoD grid of the reference and compared PC points. In the case of the coexistence of excavation and landslide, both methods reveal the change. Since the M3C2 method also gives the direction of change, it can be preferred in modeling dynamic changes like landslides. DoD method is superior to M3C2 in terms of computation time in determining the change in vertical direction such as excavation and volume calculations.

Acknowledgements

We would like to express our sincere gratitude to FİDES Mühendislik for providing access to the UAV images used in this research.

Author Contribution

Nilufer Ozdas: Conceptualization, Methodology, Data processing, Writing-Original draft preparation. **Mehmet Guven Kocak:** Conceptualization, Methodology, Data processing, Writing-Original draft preparation, Reviewing and Editing. **Serkan Karakis:** Data processing, Reviewing, and Editing.

Declaration of Competing Interests

The authors declare that they have no known relevant competing financial or non-financial interests that could have appeared to influence the work reported in this paper.

References

Besl, P. J., & McKay, N. D. (1992). A method for registration of 3-D shapes. *IEEE Transactions on Pattern Analysis and Machine Intelligence*, *14*(2), 239-256.

Cao, D., Zhang, B., Zhang, X., Yin, L., & Man, X. (2023). Optimization methods on dynamic monitoring of mineral reserves for open pit mine based on UAV oblique photogrammetry. *Measurement*, *207*, 112364.

Cook, K. L. (2017). An evaluation of the effectiveness of low-cost UAVs and structure from motion for geomorphic change detection. *Geomorphology*, *278*, 195-208.

de Gélis, I., Lefèvre, S., & Corpetti, T. (2021). Change detection in urban point clouds: An experimental comparison with simulated 3d datasets. *Remote Sensing*, *13*(13), 2629.

James, M. R., Robson, S., & Smith, M. W. (2017). 3-D uncertainty-based topographic change detection with structure-from-motion photogrammetry: precision maps for ground control and directly georeferenced surveys. *Earth Surface Processes and Landforms*, *42*(12), 1769-1788.

Kharroubi, A., Poux, F., Ballouch, Z., Hajji, R., & Billen, R. (2022). Three dimensional change detection using point clouds: A review. *Geomatics*, *2*(4), 457-485.

Lague, D., Brodu, N., & Leroux, J. (2013). Accurate 3D comparison of complex topography with terrestrial laser scanner: Application to

the Rangitikei canyon (NZ). *ISPRS journal of photogrammetry and remote sensing*, *82*, 10-26.

Li, P., Li, D., Hu, J., Fassnacht, F. E., Latifi, H., Yao, W., Gao, J., Chan, F.K.S., Dang, T., & Tang, F. (2024). Improving the application of UAV-LiDAR for erosion monitoring through accounting for uncertainty in DEM of difference. *Catena*, *234*, 107534.

Liu, X., Zhu, W., Lian, X., & Xu, X. (2023). Monitoring mining surface subsidence with multi-temporal three-dimensional unmanned aerial vehicle point cloud. *Remote Sensing*, *15*(2), 374.

Nex, F., Armenakis, C., Cramer, M., Cucci, D. A., Gerke, M., Honkavaara, E., Kukko, A., Persello, C., & Skaloud, J. (2022). UAV in the advent of the twenties: Where we stand and what is next. *ISPRS journal of photogrammetry and remote sensing*, *184*, 215-242.

Nourbakhshbeidokhti, S., Kinoshita, A. M., Chin, A., & Florsheim, J. L. (2019). A workflow to estimate topographic and volumetric changes and errors in channel sedimentation after disturbance. *Remote Sensing*, *11*(5), 586.

Okyay, U., Telling, J., Glennie, C. L., & Dietrich, W. E. (2019). Airborne lidar change detection: An overview of Earth sciences applications. *Earth-Science Reviews*, *198*, 102929.

Ren, H., Zhao, Y., Xiao, W., & Hu, Z. (2019). A review of UAV monitoring in mining areas: Current status and future perspectives. *International Journal of Coal Science & Technology*, *6*, 320-333.

Théau, J. (2022). *Change detection*. Kresse, W., & Danko, D. (ed) *Springer Handbook of Geographic Information*, Springer International Publishing.

Williams, R. (2012). DEMs of difference. *Geomorphological Techniques*, *2*(3.2).

Wilson, J. P. (2012). Digital terrain modeling. *Geomorphology*, *137*(1), 107-121.

URL-1: CloudCompare (version 2.12.4) [GPL software], http://www.cloudcompare.org/ (Accessed: 25 December 2023).